Non-Equilibrium Processes in Galaxy Cluster Accretion Shock Regions

Ka-Wah Wong[1,2], Craig L. Sarazin[2], Li Ji[3], & Daniel R. Wik[2,4]

[1]Department of Physics & Astronomy, University of Alabama, Tuscaloosa, USA; kwong@ua.edu,

[2]Department of Astronomy, University of Virginia, USA,

[3]MIT Kavli Institute for Astrophysics and Space Research, USA, [4]NASA GSFC, USA

Summary

1) Due to the long collisional ionization equilibrium (CIE) timescales, heavy elements will be under-ionized after they have passed through the accretion shock (upper left block).
2) The most prominent non-equilibrium ionization (NEI) signature is the O VII and O VIII line ratio (lower left block).
3) Depending on the line ratio measured, an exposure of ~130—380 ksec on a moderate-redshift (z≈0.03—0.1), massive regular cluster with the IXO will be sufficient to provide a strong test for the NEI model (upper right block).
4) Because of the long collisional timescale, electrons and ions in the accretion shock regions may not be in equipartition as well (Fox & Loeb 1997). Cosmological parameter estimation from SZ surveys can be biased by up to 10% (lower right block).

Non-Equilibrium Ionization (NEI) in Cluster Outer Regions:

- The densities in the outer regions of clusters of galaxies are very low ($n_e \sim 10^{-5}$ cm^{-3}), and the CIE timescales are very long (e.g., $t_{CIE} \sim 0.3$ Gyr $(n_e/10^{-5}$ cm$^{-3})^{-1}$ for O VII and even longer for heavier ions). As a result, heavy elements will be under-ionized after they have passed through the accretion shock. We have studied systematically the NEI effects for relaxed clusters in the ΛCDM cosmology using 1-D hydrodynamic simulations (Wong et al. 2011).

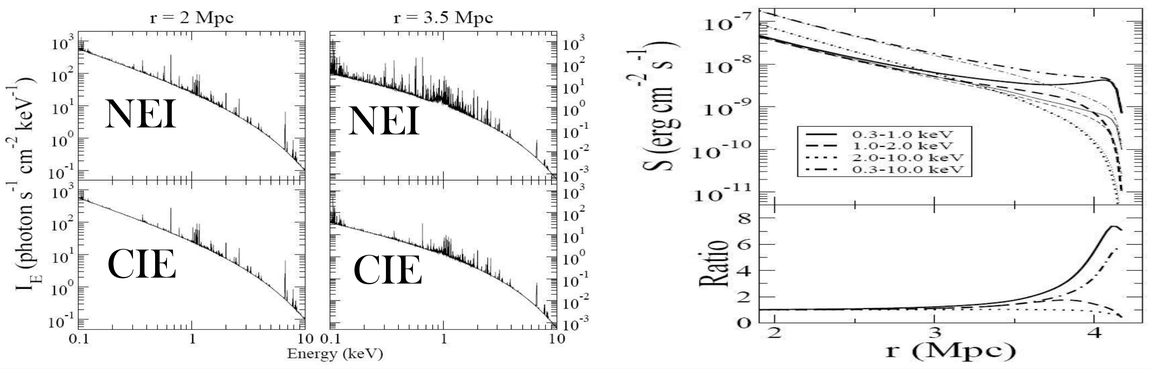

Figure 1 ***(left):*** Projected rest frame spectra at two projected radii. Upper panels: the NEI model with non-equipartition of electrons and ions. Lower panels: projected rest frame spectra for the CIE model with non-equipartition (CIE—Non-Eq). Unless otherwise specified, all cluster models are with $M_{vir} = 1.53 \times 10^{15} M_\odot$ (or $M_{200} = 1.99 \times 10^{15} M_\odot$).

Figure 2 ***(right):*** Upper panel: rest frame projected surface brightness profiles for different energy bands for the NEI model (thick lines) and the CIE—Non-Eq model (thin lines). Lower panel: ratios of the surface brightness profiles $S_{NEI}/S_{CIE\text{-}Non\text{-}Eq}$. Note: the NEI model predicts a much stronger soft emission than the CIE—Non-Eq model in the outer regions.

Non-Equilibrium Ionization Signature: O VII and O VIII Line Ratio:

- The most prominent NEI signature in the line emission is the line ratio of the He-like O VII triplets and the O VIII doubles, S(O VIII)/S(O VII).
- The electron temperature can be measured from, e.g., fits to the continuum spectra, allowing the CIE line ratios to be determined and compared to the observed ratios.
- Note that the ratios for NEI and CIE models are different by more than an order of magnitude at radii beyond half of the shock radius. A ratio < 3 is a clear NEI signature as the CIE ratios are always > 3 and almost always > 10 (Fig. 4).
- NEI signatures are equally strong for different non-adiabatic shock electron heating efficiency β.

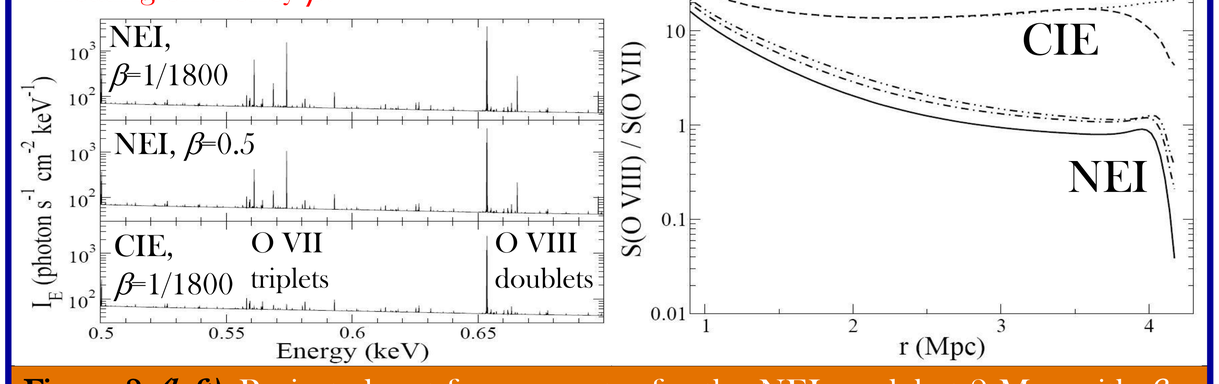

Figure 3 ***(left):*** Projected rest frame spectra for the NEI model at 2 Mpc with β = 1/1800 (upper panel) and β = 0.5 (middle panel). Lower panel is for the CIE—Non-Eq model with β = 1/1800.

Figure 4 ***(right):*** Line ratios S(O VIII)/S(O VII) for the NEI models with β = 1/1800 (solid), 0.5 (dash-dotted), and 1.0 (dash-dot-dotted). Line ratios for the CIE—Non-Eq (dashed) and CIE—Eq (dotted) models are also shown.

Testing the Non-Equilibrium Ionization Signature with IXO:

- An observation of a moderate-redshift ($z \approx 0.03$—0.1), massive ($M_{200} \gtrsim 10^{15} M_\odot$) regular cluster with about 130 [220] ksec with the IXO X-ray Microcalorimeter Spectrometer (XMS) full [core] array is enough to measure the line ratio at 2.3-σ. For a 3-σ measurement of the line ratio, about 230 [380] ksec will be needed for the XMS full [core] array. Note that because of the order of magnitude difference in the NEI and CIE line ratios, a 2 or 3-σ measurement in line ratio can be sufficient to rule out CIE model (see the discussions in Wong et al. 2011).

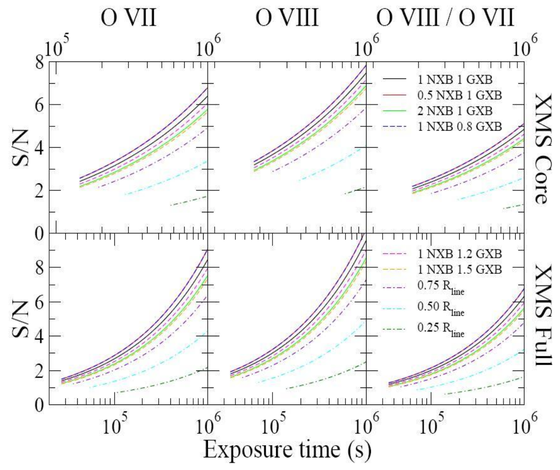

Figure 5: Left (middle) panels show the signal-to-noise ratios for the O VII triplets (O VIII doublets) expected to be detected by IXO. The right panels show the signal-to-noise ratios for the O VII and O VIII line ratios. The upper panels correspond to the XMS core array, and the lower panels correspond to the XMS full array. Different signal and noise levels are assumed for the different models.

Impacts of Non-Equipartition on Cosmological Parameter Estimation from SZ surveys:

- Hydrodynamic simulations show that non-equipartition effect can introduce a ~5—10% bias to the SZ effect at around R_{vir} (Rudd & Nagai 2009; Wong & Sarazin 2009).
- Using the technique developed by Randall et al. (2002) and Wik et al. (2008), we generated the SZ integrated Y functions with the non-equipartition model using the analytic Press-Schechter theory. We then fitted the generated Y functions with the biased Y-M relation if non-equipartition effect is not properly taken into account. We found that depending on calibration methods, non-equipartition effects can introduce up to ~10% bias in cosmological parameter measurements (Table 1; Wong et al. 2010).

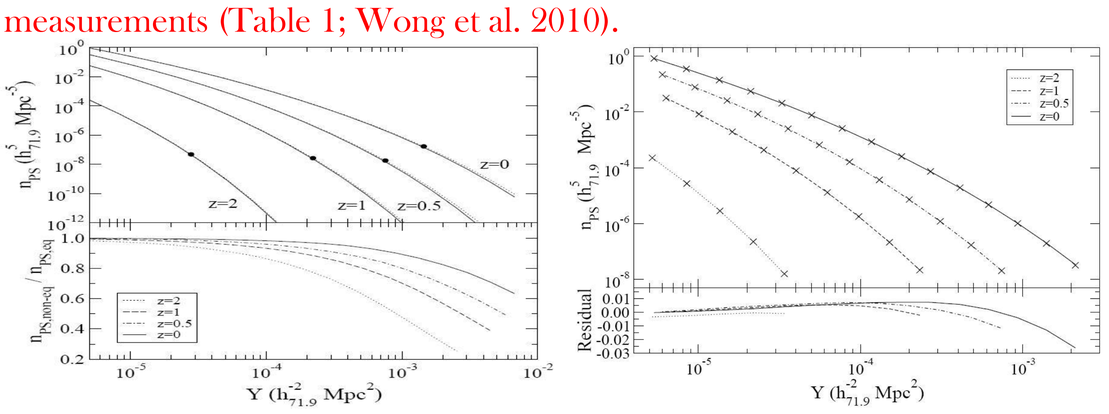

Figure 6 ***(left):*** Top: Integrated Y functions of the non-equipartition (solid lines) and the equipartition (dotted lines) models in the ΛCDM universe. Solid dots indicate $n_{PS} Y \Delta V$=1, where ΔV is the comoving volume element between the reshifts. Bottom: Ratios between the non-equipartition and the equipartition Y functions.

Figure 7 ***(right):*** Top: Biased Y functions in *Case 2* (crosses) and the best fitted Y functions (lines). The dark energy equation of state parameter w ($=w_0+w_1 z/(1+z)^2$) is frozen to be -1 in the fitting. Bottom panel: Residual given by the logs in the biased Y functions minus the logs in the best fit Y functions.

Table 1: Best-fit cosmological parameters with different potential systematic uncertainties. The assumed cosmological parameters are $\Omega_M = 0.258$, $\sigma_8 = 0.796$, $w_0 = -1$, and $w_1 = 0$. The squared bracketed values are the frozen values in the fits. The round bracketed values in column 2, 3, and 4 are the percentage deviations of the fitted cosmological parameters from the assumed parameters. The round bracketed values in column 5 are the largest percentage change in w occur between the present time ($z = 0$) and $z = 2$, and that change is $w = w_1/4$.

Calibration	Ω_M	σ_8	w_0	w_1
Case 1	0.2548(-1.2%)	0.7950(-0.1%)	[-1]	[0]
	0.2665(+3.3%)	0.7830(-1.6%)	-0.9464(-5.4%)	[0]
	0.2680(+3.9%)	0.7811(-1.9%)	-0.9031(-9.7%)	-0.2362(+5.9%)
Case 2	0.2579(0%)	0.7976(+0.2%)	[-1]	[0]
	0.2602(+0.9%)	0.7951(-0.1%)	-0.9890(-1.1%)	[0]
	0.2610(+1.2%)	0.7940(-0.3%)	-0.9577(-4.2%)	-0.1725(+4.3%)
Case 3	0.2585(+0.2%)	0.7953(-0.1%)	[-1]	[0]
	0.2604(+0.9%)	0.7932(-0.4%)	-0.9910(-0.9%)	[0]
	0.2601(+0.2%)	0.7938(-0.3%)	-1.0123(+1.2%)	0.1167(-2.9%)

References

Fox, D., & Loeb, A. 1997, ApJ, 491, 459

Randall, S. W., Sarazin, C. L., & Ricker, P. M. 2002, ApJ, 577, 579

Rudd , D. H., & Nagai, D. 2009, ApJ, 701, L16

Wik, D. R., Sarazin, C. L., Ricker, P. M., & Randall, S. W. 2008, ApJ, 680, 17

Wong, K.-W., & Sarazin, C. L. 2009, ApJ, 707, 1141

Wong, K.-W., Sarazin, C. L., & Wik, D. R. 2010, ApJ, 719, 1

Wong, K.-W., Sarazin, C. L., & Ji, L. 2011, ApJ, 727, 126